2. J.S. Hong and M.J. Lancaster, Microstrip filters for RF/microwave applications, Wiley, New York, 2001.
3. M. Makimoto and S. Yamashita, Bandpass filters using parallel coupled stripline stepped impedance resonators, IEEE Trans Microwave Theory Tech 28 (1980), 1413–1417.
4. G. Adnan, A novel dual-mode bandpass filter with wide stopband using the properties of microstrip open-loop resonator, IEEE Microwave Wireless Components Lett 12 (2002), 386–389.
5. C.W. Tang and H.H. Liang, Parallel-coupled stacked SIRs bandpass filters with open-loop resonators for suppression of spurious responses, IEEE Microwave Wireless Components Lett 15 (2005), 802–805.
6. W.H. Tu and K. Chang, Compact microstrip bandstop filter using open stub and spurline, IEEE Microwave Wireless Components Lett 15 (2006), 268–270.
7. W.H. Tu and K. Chang, Compact second harmonic-suppressed bandstop and bandpass filters using open stubs, IEEE Trans Microwave Theory Tech 54 (2006), 2497–2502.
8. X.D. Huang and C.H. Cheng, A novel microstrip dual-mode bandpass filter with harmonic suppression, IEEE Microwave Wireless Components Lett 16 (2006), 404–406.
9. W.R. Eisenstadt, B. Stengel, and B.M. Thompson, Microwave differential circuit design using mixed-mode S-parameters, Artech house, Boston, MA, 2006, pp. 1–25
10. S.G. Kim and K. Chang, Ultrawide-band transitions and new microwave components using double-sided parallel-strip lines, IEEE Trans Microwave Theory Tech 52 (2004), 2148–2152.

A NOVEL MINIATURIZED TRIBAND PIFA FOR MIMO APPLICATIONS

Majid Manteghi and Yahya Rahmat-Samii
Department of Electrical Engineering, Antenna Research and Measurements Laboratory, University of California, Los Angeles, CA 90095-1594

Received 23 July 2006

ABSTRACT: *Multiband antennas are vital in meeting the modern telecommunication demands of mobile terminals. Using the spatial properties of multipath channels, multiple-input multiple-output (MIMO) communication systems employ antenna arrays to increase their communication capacity. This article presents a novel printed inverted "F" antenna (PIFA), which has been used to design a miniaturized triband antenna. In turn, the triband antenna has been used as an element in various arrays of MIMO applications. Specifically, the antenna element has been constructed and applied, in arrays of two and four, in a laptop PCMCIA wireless LAN card. The size of the four element MIMO antenna array is 50 mm × 13 mm × 8 mm, which translates to 0.4λ × 0.1λ × 0.06λ at 2.45 GHz. The input impedance of the single element antenna has been measured at UCLA. The antenna has a return loss lower than −10 dB within the 2.4–2.5 GHz, 5.15–5.35 GHz, and 5.7–5.85 GHz bands. The measured scattering matrices of two and four element arrays have been used to calculate the total active reflection coefficient (TARC). TARC has been calculated for different combinations of excitation signals applied at each port. Each excitation signal has a unity magnitude and a random phase, thus leading to innumerable signal combinations. Our results reveal that "off" diagonal elements of the scattering matrix (couplings between elements) are as important as diagonal elements in calculating the TARC and the radiation efficiency of arrays. Furthermore, increasing the number of elements in a MIMO system with a limited volume will increase the channel capacity but lower the radiation efficiency. The experimental and simulation results have been in agreement.* © 2007 Wiley Periodicals, Inc. Microwave Opt Technol Lett 49: 724–731, 2007; Published online in Wiley InterScience (www.interscience.wiley.com). DOI 10.1002/mop.22239

Key words: *MIMO; multi-band antenna; printed inverted "F" antenna; scattering matrix; channel capacity*

1. INTRODUCTION

Printed inverted "F" antenna (PIFA) designs [Fig. 1(a)] have low profiles, good radiation characteristics, and wide bandwidths [1–3]. This makes PIFA an attractive choice for antenna designs targeting various mobile wireless systems. However, the higher order resonant frequencies of the standard PIFA design are not within the range of its fundamental resonant frequency. This discrepancy between frequencies results in a single band antenna [Fig. 1(b)]. In addition, both the radiation performance and the return loss of a standard PIFA may render it inefficient for use at higher order resonant frequencies.

A requirement of many modern communication systems is support of multiple resonant frequencies. Therefore, the PIFA structure has to be modified to achieve additional resonant frequencies. It has been demonstrated that a PIFA can resonate at a second frequency by adding a properly placed slot on the antenna body [4]. In fact, different shapes and locations of slots have been proposed for diverse applications [5, 6]. The most popular form is the dual frequency PIFA which employs a J-shape slot [7, 8]. The J-shaped slot unequally divides the standard PIFA into two new PIFAs, connected in parallel [Fig. 2(a)]. The smaller PIFA can be treated as an independent antenna. The properties of the smaller PIFA, with the higher resonant frequency, can be altered by varying the shape and the size of the J-shaped slot. Noticeably, the two PIFAs reactively load one another.

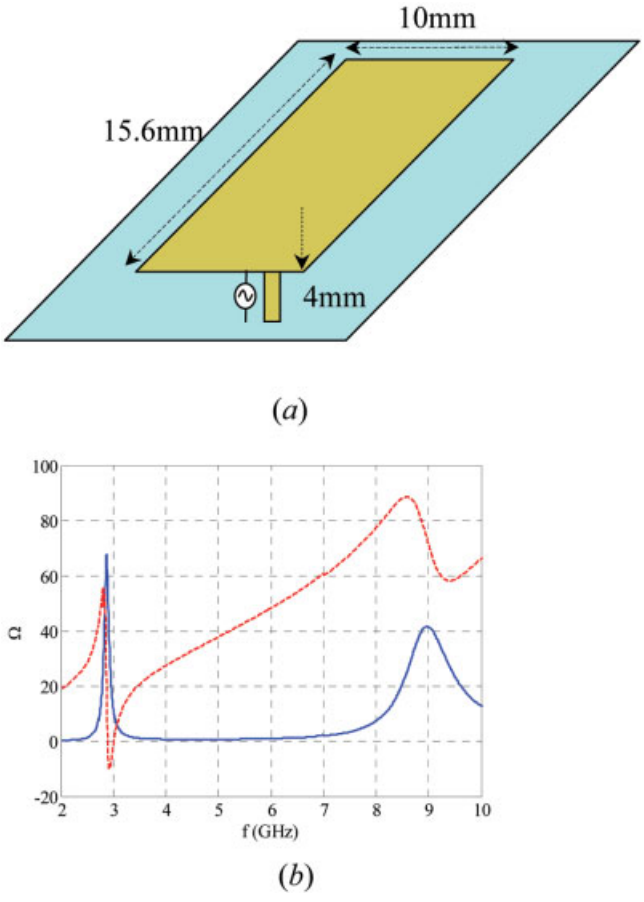

Figure 1 (a) Basic 15.6 mm × 10 mm PIFA 4 mm above the ground plane. (b) real and imaginary part of the input impedance. [Color figure can be viewed in the online issue, which is available at www.interscience.wiley.com]

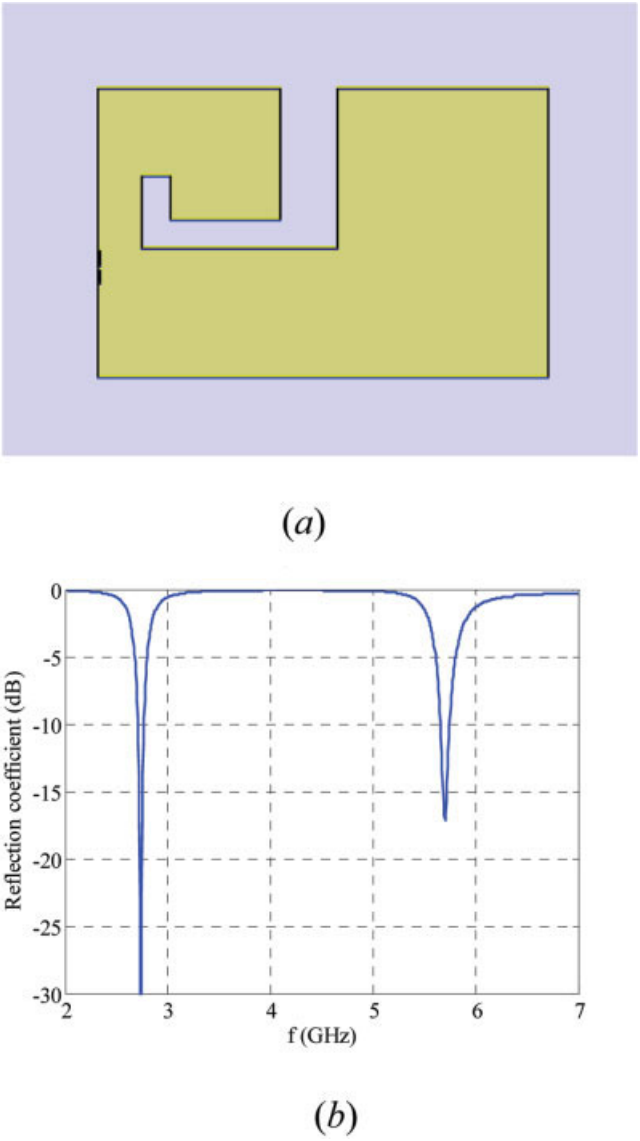

Figure 2 (a) Dual-band PIFA using a J-shaped slot. (b) Reflection coefficient of the dual-band PIFA. [Color figure can be viewed in the online issue, which is available at www.interscience.wiley.com]

This article is aimed toward a novel miniaturized triband single-feed PIFA, for WLAN applications, which operates in the 2.4–2.5 GHz, 5.15–5.35 GHz, and 5.7–5.85 GHz frequency bands. A PIFA can be designed with a J-shaped slot that supports the first and the second frequency bands mentioned. Increasing the height of this PIFA will improve the frequency bandwidth, enabling its support of the third frequency band [9]. A developing issue, however, is the increased coupling between the array elements because of the increased height of the PIFA. This effect decreases the radiation efficiency of the array system. As such, the maximum achievable height of the PIFA is limited. Moreover, the radiation from the induced current on the feeding cables could generate further issues for the height-increased PIFA, in a small ground plane [9]. It is problematic to add another J-shaped slot to the antenna body in order to generate the third frequency band as it will result in a shift in the second frequency band. High coupling between the two small PIFAs does not allow them to function as two independent antennas. Therefore, a PIFA with two J-shaped slots can support only three rather apart frequency bands [10].

Subsequently, a novel triband PIFA is presented. The proposed antenna is simulated by Ansoft HFSS and the results are compared with antenna's measurements in Section III. Arrays of two and four elements are studied for MIMO application and the results are presented in Section 4. Section 5 concludes the article.

2. MINIATURIZED TRIBAND PIFA

Figure 1(a) displays a 10 mm × 15.6 mm × 4 mm standard PIFA located at the corner of a 50 mm × 100 mm ground plane. This antenna has been used as the key element in our designs. Figure 3(a) contains the calculated current distribution on the antenna body, at the resonant frequency. As demonstrated, the vicinity of the shorting pin has the maximum current density. Figure 3(b) presents the calculated electric field intensity on a plane normal to the antenna body, at the resonant frequency. This figure illustrates that the furthest edge of the PIFA has the highest electric field intensity. According to Figure 3(a), the feeding point of a standard PIFA is close to the shorting pin with the high current density.

To divide this standard PIFA into two parallel PIFAs a second antenna with similar current distribution and field intensity is required at the second resonant frequency. As the first step a J-shaped slot is added to the antenna body [Fig. 2(a)]. The calculated reflection coefficient of the dual-band PIFA is depicted in Figure 2(b). The change in the antenna structure, due to addition of the J-shaped slot, has shifted the first resonant frequency. The calculated current distributions on the antenna body, for both

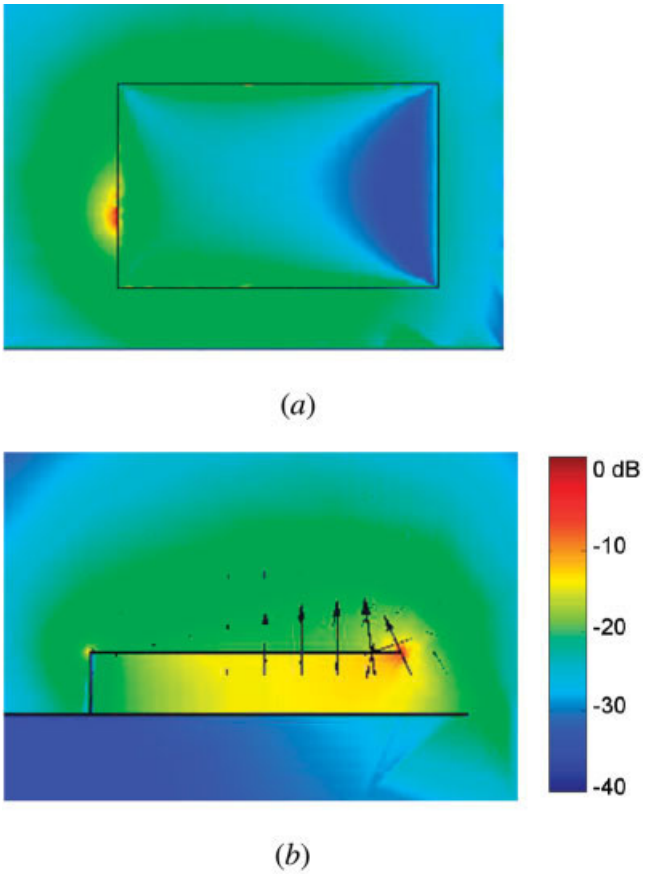

Figure 3 (a) Calculated current distribution on the antenna at 2.89 GHz (resonant frequency). (b) Calculated electric field intensity of the PIFA in a plane normal to the antenna body at 2.89 GHz. [Color figure can be viewed in the online issue, which is available at www.interscience.wiley.com]

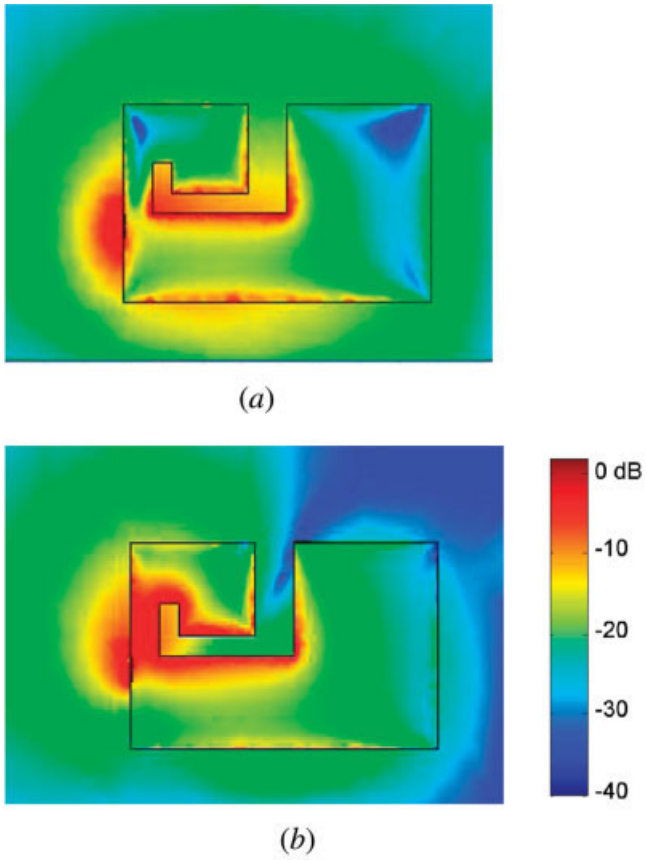

Figure 4 (a) and (b) calculated current distribution on the dual-band PIFA at 2.74 and 5.7 GHz, respectively. [Color figure can be viewed in the online issue, which is available at www.interscience.wiley.com]

resonant frequencies, are represented in Figure 4. Similar to the standard PIFA, at both resonant frequencies, the current distribution has a maximum close to the shorting pin. For both resonant frequencies, the electric field intensities on the planes normal to the dual-band PIFA are presented in the Figure 5. These figures clearly demonstrate that for both PIFAs, at their resonant frequencies, the edges furthest from the feeding point have the maximum field intensities. Furthermore, at their resonant frequencies, each antenna affects the other's current distribution and electric field intensity. Provided that resonant frequencies are not in close range, each antenna functions as an independent antenna that is loaded by the accompanying antenna. Using the same strategy, adding more PIFAs in parallel is possible if their resonant frequencies are adequately separated.

To generate the third resonant frequency, a quarter wavelength slot is added to the dual-band PIFA structure. The assembled PIFA has resonant frequencies at 2.45, 5.25, and 5.775 GHz with supporting bandwidths of 100, 200, and 150 MHz, respectively. This triband, single element, antenna model, and its calculated and measured reflection coefficients, are shown in Figure 6. Adding the third resonant frequency shifts the first and second resonant frequencies. The first resonant frequency adjusts as the portion of the antenna, which was associated with this resonant frequency, was modified. The shift in the second resonant frequency is due to the coupling between the quarter wavelength slot and the small PIFA. Our simulation results verify that the two resonant frequencies can be as closely tuned as desired.

Figure 7 exhibits the calculated current distributions on the body of the triband PIFA, at its three resonant frequencies. It is apparent that the small PIFA and the quarter wavelength slot antenna load the large PIFA (lowest frequency) as two open ended transmission lines. The smaller PIFA is parallel at the feeding point and the quarter wavelength slot is in series. Each section of the triband antenna carries a maximum current at its resonant frequency.

3. ARRAY OF TRIBAND PIFAs FOR MIMO APPLICATIONS: TWO AND FOUR ELEMENT ARRAYS

The achievable spectral efficiency of multiple antenna radios is greatly improved by multiple-input multiple-output (MIMO) systems. There is a limited volume assigned to the antenna system in most portable devices ($0.4\lambda \times 0.1\lambda \times 0.06\lambda$ at 2.45 GHz for our system). Therefore, a miniaturized antenna is required as the element of the array for these applications. Yet, the complication with small element spacing is the mutual coupling between the elements. Mutual coupling disrupts the isolated state characteristics of the scattering parameter and radiation pattern of the array's radiating elements [11, 12]. In the following paragraphs it will become evident that mutual coupling reduces the radiation efficiencies of the arrays. Thus, it is necessary for the elements in a MIMO antenna array to be designed collectively. More importantly, a PIFA is relatively robust to influence from another nearby PIFA due to the radiating element's low profile and proximity to the ground plane [13].

3.1. Two-Element MIMO Design

A two-element PIFA array (Fig. 8) was designed for use in MIMO enabled portable devices, based on the proposed triband PIFA

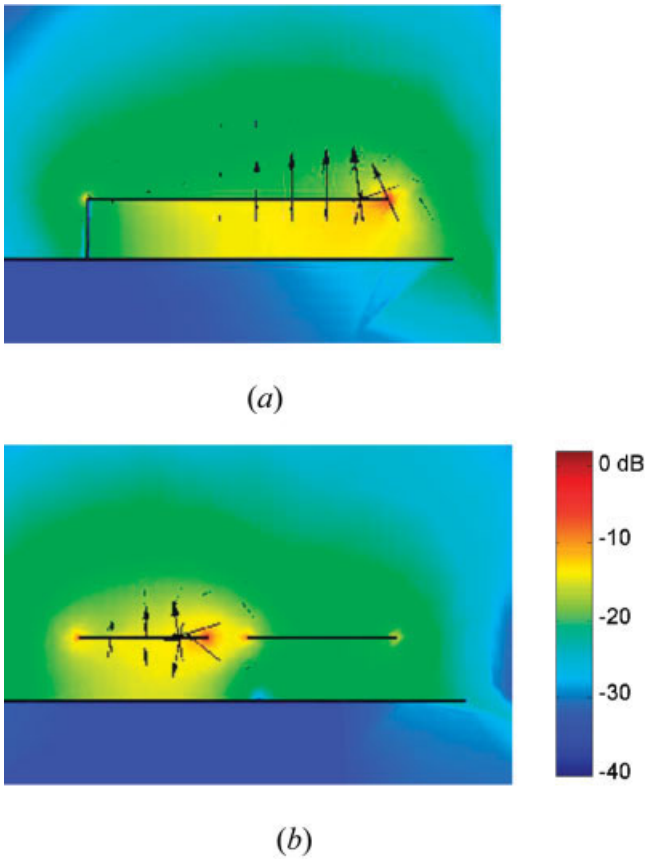

Figure 5 (a) and (b) calculated electric field intensity in a plane normal to the antenna at 2.74 and 5.7 GHz, respectively. [Color figure can be viewed in the online issue, which is available at www.interscience.wiley.com]

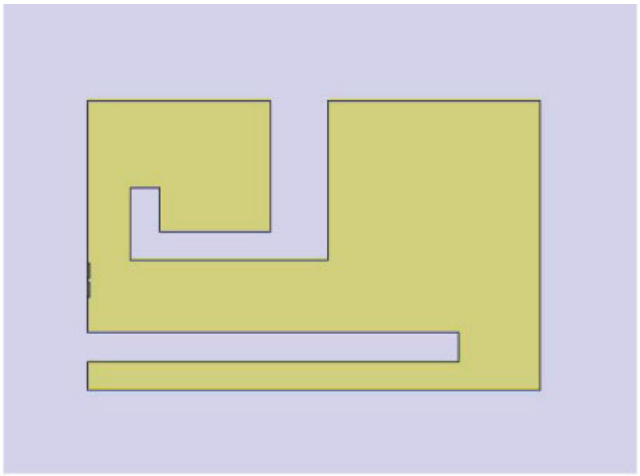

(a)

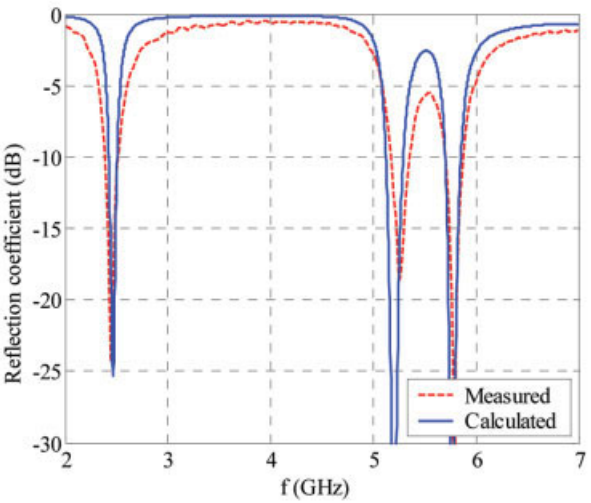

(b)

Figure 6 (a) Triband PIFA with a J-slot and a quarter wavelength slot. (b) calculated and measured return loss of the triband antenna. [Color figure can be viewed in the online issue, which is available at www.interscience.wiley.com]

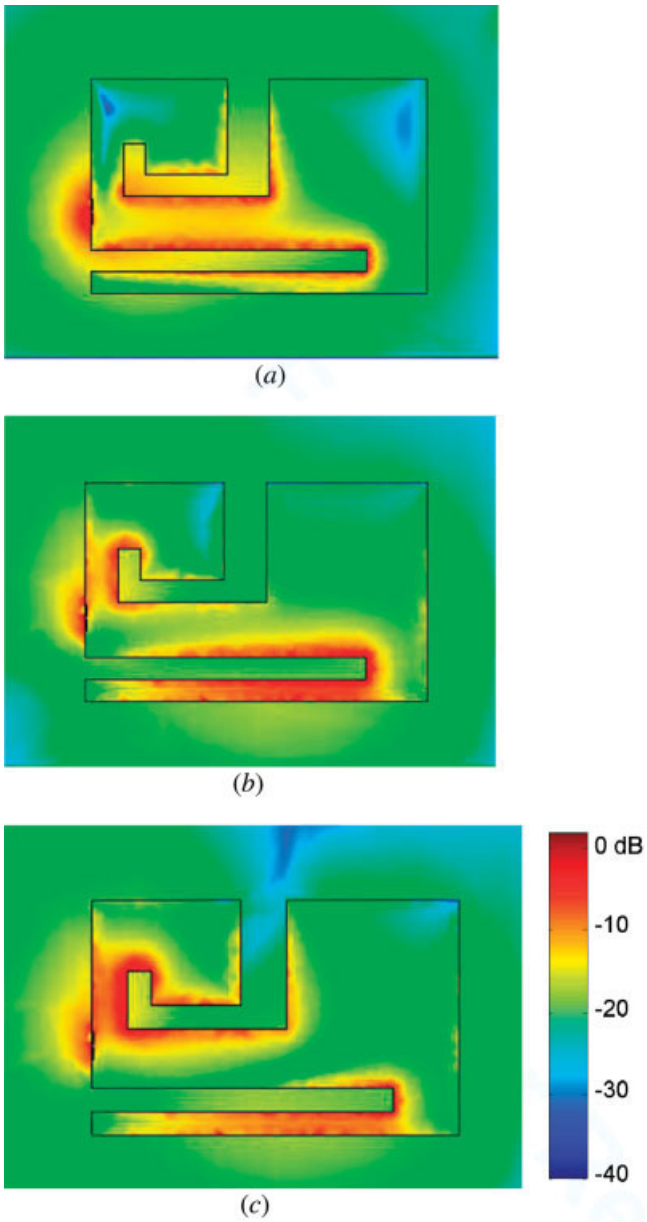

(a)

(b)

(c)

Figure 7 Calculated current distribution of the triband antenna at (a) 2.45 GHz, (b) 5.23 GHz, and (c) 5.75 GHz. [Color figure can be viewed in the online issue, which is available at www.interscience.wiley.com]

[14]. The PIFA array's elements were separated by 31 mm. An Ansoft high frequency structure simulator software package (HFSS) was employed to calculate the input impedance and the far-field patterns of this array. Figure 9 contains the far-field patterns of a single PIFA sharing a ground plane with a second PIFA (placed 31 mm away, Fig. 8) and terminated by a 50 Ω load. These far-field patterns are given for two elevation planes ($\varphi = 0°$ and $\varphi = 90°$) and the azimuth plane ($\theta = 90°$). A comparison of Figures 9(a) and 9(b) reveals that the radiation pattern of a single PIFA remains relatively unchanged in the presence of a second PIFA.

Figure 10 presents the scattering matrix of the dual element PIFA array as a function of frequency. It has been shown that the diagonal elements of the scattering matrix, s_{ii}, do not well characterize the radiation efficiency of a multiport antenna [15]. A portion of the power accepted by each element disperses to other ports via mutual coupling between the elements. This coupling is

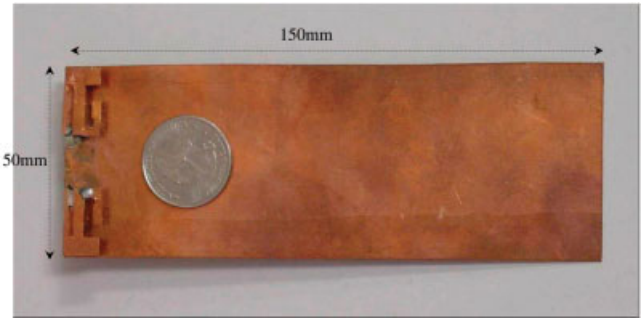

Figure 8 Array of two elements of triband PIFA. [Color figure can be viewed in the online issue, which is available at www.interscience.wiley.com]

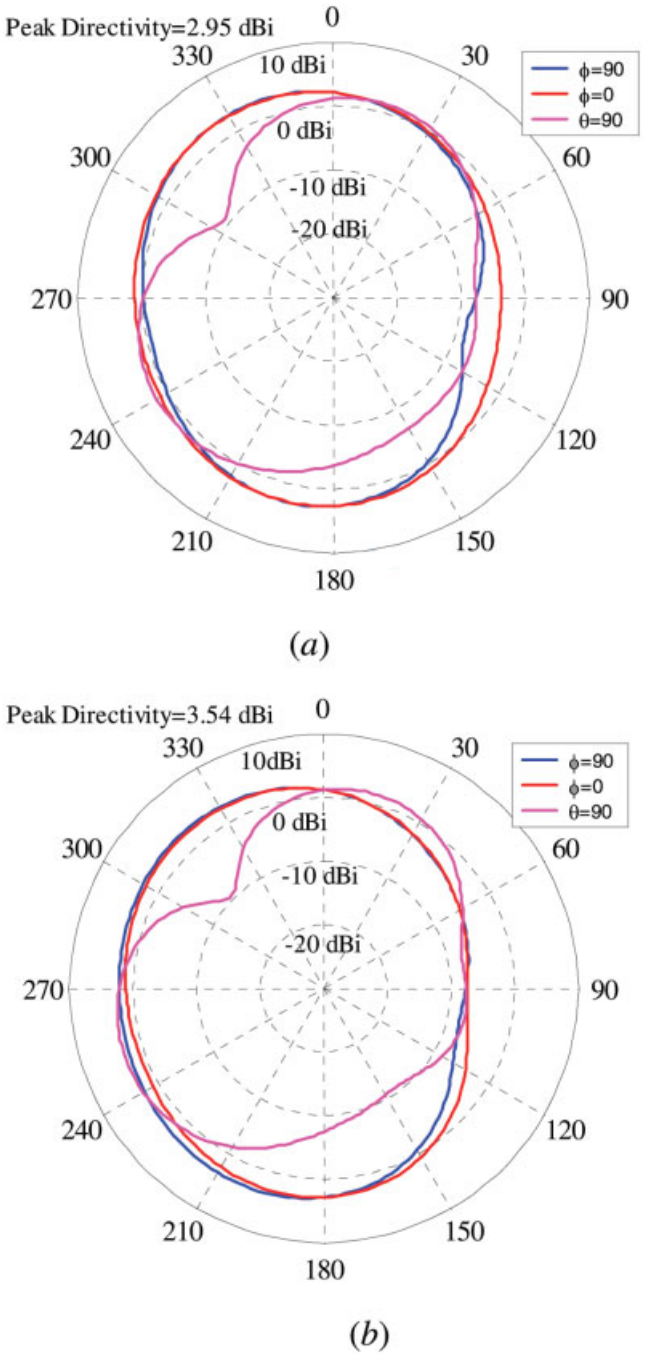

Figure 9 (a) Calculated far field azimuth and elevation patterns at 2.45 GHz for the single PIFA. (b) Calculated far field azimuth and elevation patterns at 2.45 GHz for the single PIFA in presence of the second element. [Color figure can be viewed in the online issue, which is available at www.interscience.wiley.com]

best characterized by the "off" diagonal elements, s_{ij}, of the scattering matrix. The combination of an antenna port's primary reflected signal with the coupled signals can be constructive or destructive depending on the phase of the component signals. Each antenna in a wideband MIMO transmitter is subjected to a randomly phased excitation signal. The signal phases are randomized by the propagation environment prior to reaching the receiver. The efficiency of the MIMO antenna is a function of combinations of randomly phased signals. The efficiency cannot be determined from the traditional scattering matrix characterization.

A more effective measure of the MIMO antenna efficiency is the total active reflection coefficient (TARC) [15], which is ratio of the square root of the total reflected power divided by the square root of the total incident power. The TARC calculated for a *N*-port antenna system, $[b] = [Sp][a]$, where a_i is the incident signal vector, b_i is the reflected signal vector and *Sp* is the scattering matrix of the *N*–port antenna system. TARC can be calculated as

$$\Gamma_a^t = \frac{\sqrt{\sum_{i=1}^{N} |b_i|^2}}{\sqrt{\sum_{i=1}^{N} |a_i|^2}}. \quad (1)$$

One can calculate the radiation efficiency of a lossless antenna as

$$\eta(\%) = 100 \times (1 - |\Gamma_a^t|^2) = 100 \times \left(\frac{\sum_{i=1}^{N} (|a_i|^2 - |b_i|^2)}{\sum_{i=1}^{N} |a_i|^2} \right). \quad (2)$$

The TARC has been calculated for different combinations of excitation signals applied to each port. Each excitation signal has a unity magnitude and a random phase. The random phasing of the excitation signals probes the array so as to cause constructive (worst case) or destructive (best case) combination of coupled signals with the primary reflected signal. These excitation signals more accurately simulate wideband MIMO signaling than signals characterizing the scattering matrix. Of note, signals combine linearly (voltages) whereas the resulting power signal, used in computing TARC, add as the squared magnitude of the voltage signals. Therefore, TARC increases quickly as the number of array elements increase.

The TARC of the two-element PIFA array was calculated using twenty excitation vectors. The results are presented in Figure 11. The calculated TARC is less than −9 dB for the numerous excitation vector combinations. Demonstrably, the array has high efficiency across a range of possible MIMO signals.

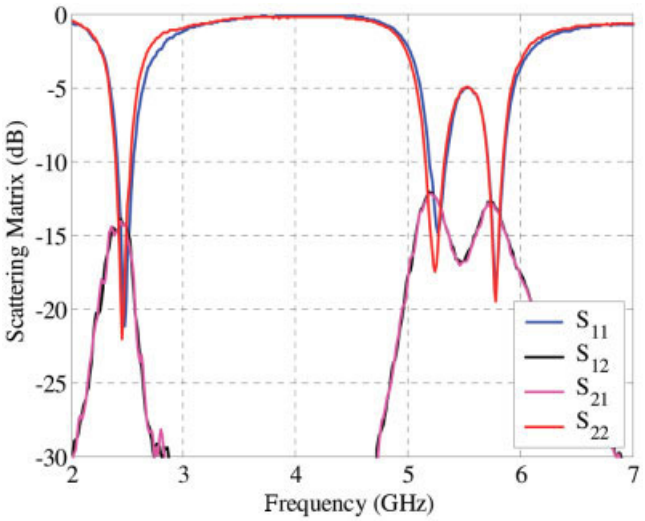

Figure 10 Measured scattering matrix for the dual PIFA array. [Color figure can be viewed in the online issue, which is available at www.interscience.wiley.com]

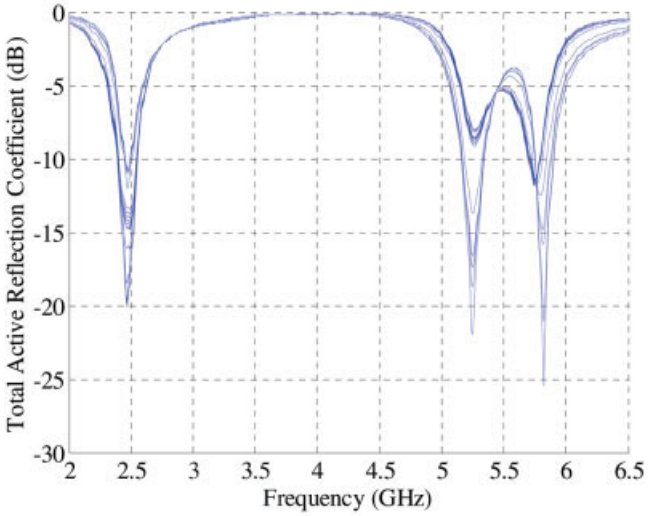

Figure 11 TARC for the 2-element PIFA array. Each curve represents calculated TARC from the measured data where the antennas were excited at the same amplitude but with a random phase. [Color figure can be viewed in the online issue, which is available at www.interscience.wiley.com]

3.2. *Four-Element MIMO Design*

The design for the two-element PIFA array was adapted to construct a four-element array by using both sides of the ground plane. The volume occupied by the four PIFAs measures 50 mm × 13 mm × 8 mm. Figure 12 exhibits two perspectives of the manufactured four-element PIFA array. Two RT-Duroid substrates are attached back-to-back to constitute four microstrip lines that feed the array's elements. Because of the small distance between top and bottom elements, a high level of mutual coupling can be expected between elements 1 and 3 and between elements 2 and 4. However, lower mutual coupling can be expected between elements 2 and 3 and between elements 1 and 4. Figure 13 delineates a row of the scattering matrix of the four-element PIFA array. The TARC of the four-element PIFA array was calculated using four excitation vectors with random phases. The TARC is less than −3 dB (efficiency higher than 50%) for the multiple excitations, as presented in Figure 14. In comparing the TARCs in Figures 11 and 14, it is apparent that TARC increases rapidly with the number of elements. Furthermore, matching networks or intermediate circuits can reduce the magnitude of the "off" diagonal elements of the array's scattering matrix, helping to reduce the TARC and increasing the antenna's efficiency.

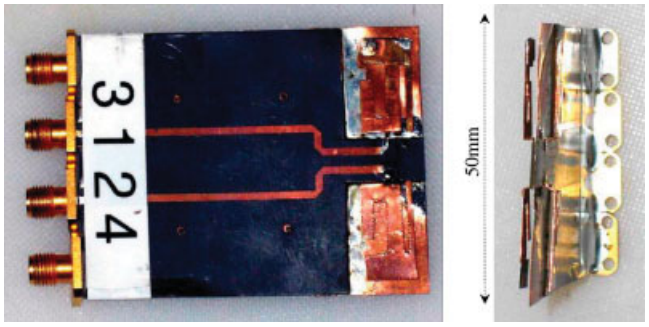

Figure 12 Four element triband PIFA constructed on two side of the ground plane. [Color figure can be viewed in the online issue, which is available at www.interscience.wiley.com]

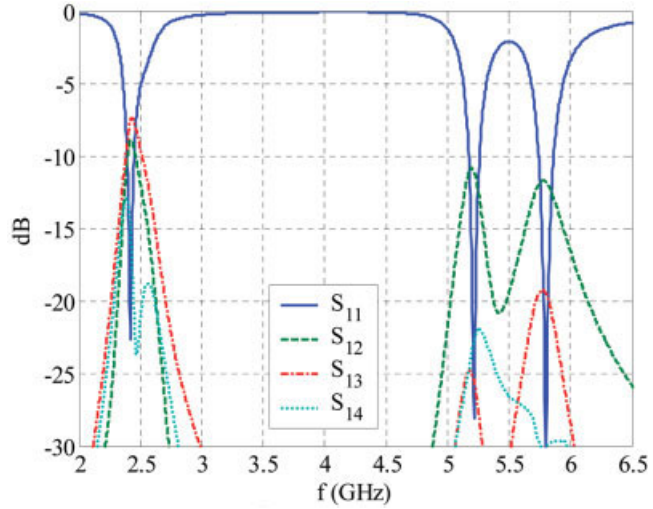

Figure 13 Calculated first row of the scattering matrix of the four element array. [Color figure can be viewed in the online issue, which is available at www.interscience.wiley.com]

Once such method is proposed in [16]. Separated ground planes have been proposed to limit the induced current on the ground plane and to reduce the mutual coupling between the antenna elements [17]. The HFSS model of four element array with separated ground plane is presented in Figure 15. Each PIFA is mounted on a small ground plane separated from the main ground plane by 1 mm. Figure 16 contains the calculated first row of the scattering matrix for this array. The TARC is calculated for 20 sets of excitations with random phase (Fig. 17). It is apparent that separation between the ground planes does not reduce the TARC. In effect the small spacing between the top and bottom antennas produces high mutual coupling.

We used the compact MIMO antenna system in a measurement setup, in a practical reach scattering environment, to measure the channel capacity for various scenarios [18]. A linear array of four dipoles, with the element spacing of 120 mm, was used in the

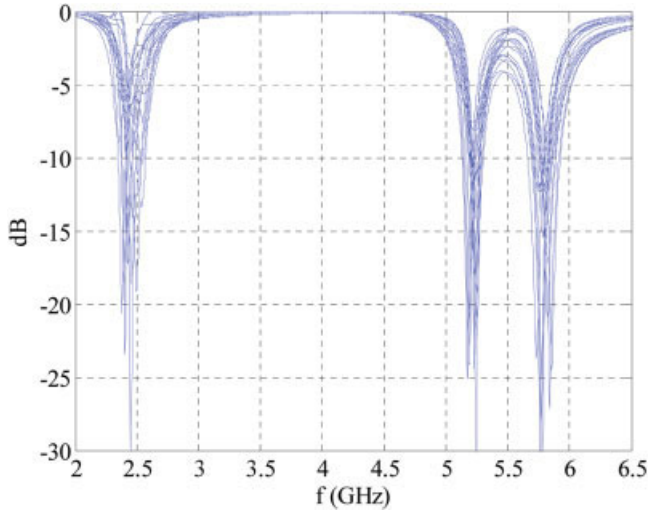

Figure 14 TARC for the four-element PIFA array. Each curve represents calculated TARC from the calculated data where the antennas were excited at the same amplitude but with a random phase. [Color figure can be viewed in the online issue, which is available at www.interscience.wiley.com]

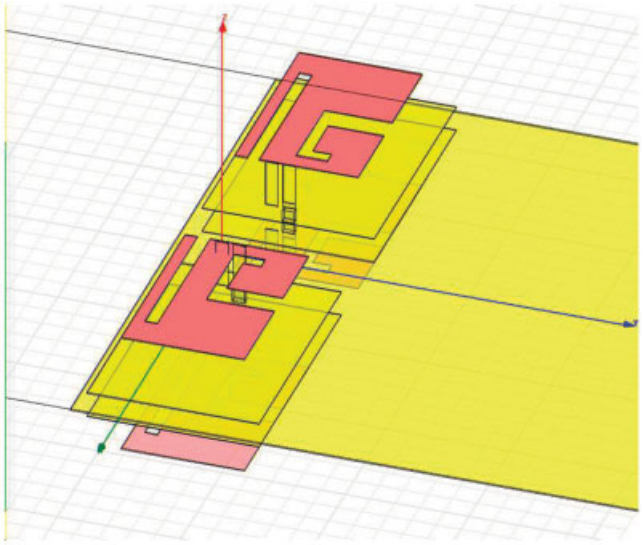

Figure 15 Four element array with separated ground plane. each element has its own ground plane which has 1 mm separation from the main ground plane. [Color figure can be viewed in the online issue, which is available at www.interscience.wiley.com]

transmitter side. The purposed compact four-element array was used in the receiver side. Since we only had radios for the 2.45 GHz band all the channel capacity were measured at 2.49 GHz. The results for various test setups are presented in the Figure 18. Furthermore, the calculated average capacities for corresponding i.i.d. Gaussian MIMO channels are plotted as solid curves. One can observe from this figure that a MIMO system with our compact array has the channel capacity close to the theoretical results.

4. CONCLUSION

A miniaturized triband PIFA was presented. The resulting PIFA has resonant frequencies at 2.45, 5.25, and 5.775 GHz with supporting bandwidths at 100, 200, and 150 MHz, respectively. The current distributions on the antenna body and the electric field

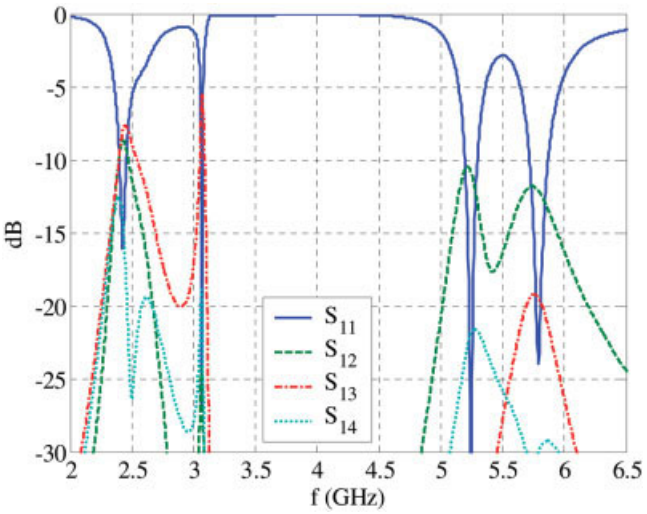

Figure 16 Calculated first row of the scattering matrix of the four element array with separated ground plane. There is an extra resonant frequency at 3.05 GHz which is associated with the small ground plane. [Color figure can be viewed in the online issue, which is available at www.interscience.wiley.com]

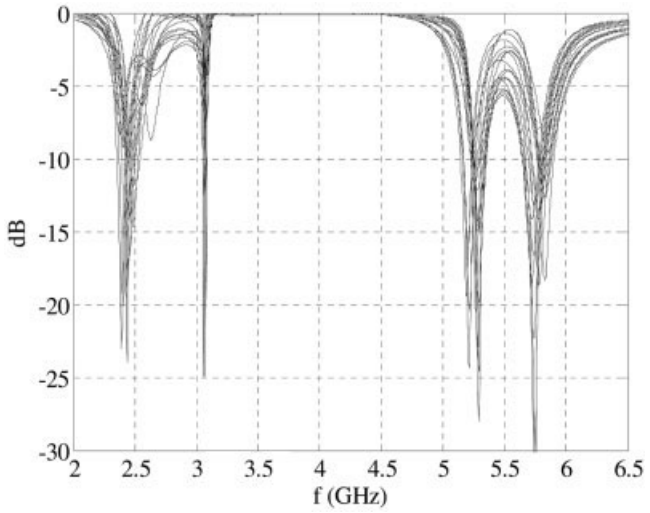

Figure 17 TARC for the four-element PIFA array with separated ground plane. Each curve represents calculated TARC from the calculated data where the antennas were excited at the same amplitude but with a random phase

intensities on the antenna plane of the antenna, at its three resonant frequencies, have been studied using the simulation results. The proposed antenna has been used in arrays of two- and four-elements, on a 50-mm width ground plane. As the volume allocated to the antenna system is $0.4\lambda \times 0.1\lambda \times 0.05\lambda$ at the lowest resonant frequency (2.45 GHz), the element spacing is 0.25λ.

The scattering matrix of the antenna was calculated and measured for both array types. The antenna arrays were excited via unit magnitude sources with random phasing to realize all possible excitation configurations. The total active reflection coefficient (TARC) was calculated for all configurations. It has been shown that all elements of the scattering matrix have equal role in the

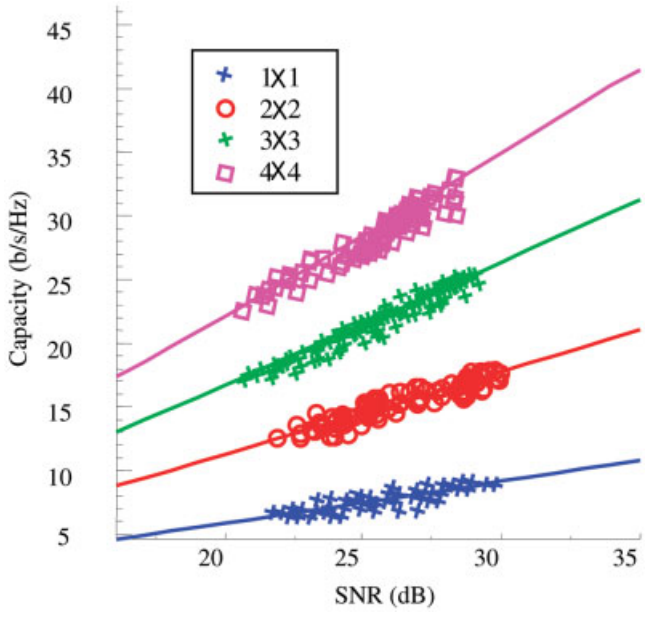

Figure 18 Measured channel capacity in an empty hall for an array of dipoles in the transmit side and the PIFA array in the receive side at 2.49 GHz. The element spacing for the dipole array is 120 mm. Average capacities for corresponding i.i.d. Gaussian MIMO channels are plotted as solid curves. [Color figure can be viewed in the online issue, which is available at www.interscience.wiley.com]

calculation of the radiation efficiency. Therefore, increasing the number of elements of an array, in a limited volume, may rapidly reduce the radiation efficiency. Our calculations confirm that TARC is always less than −9 dB for a two-element array. The same calculation for the four-element array shows that TARC is less than −3 dB for different excitations. Therefore, in the worst case consideration, 50% of the available power is radiated by the antenna array and the remainder is reflected back to the source. This suggests that there may be a need for matching network to modify the total scattering matrix.

REFERENCES

1. T. Taga and K. Tsunekawa, Performance analysis of a built-in planar inverted f antenna for 800 mhz band portable radio units, IEEE Trans Sel Areas Commun 5 (1987), 921–929.
2. M.A. Jensen and Y. Rahmat-Samii, FDTD analysis of PIFA diversity antennas on a hand-held transceiver unit, IEEE Antennas Propag Symp Dig Atlanta, GA (1993), 814–817.
3. K.L. Virga and Y. Rahmat-Samii, Low-profile enhanced-bandwidth PIFA antennas for wireless communications packaging, IEEE Trans Microwave Theory Tech 45 (1997), 1879–1888.
4. Z.D. Liu, P.S. Hall, and D. Wake, Dual-frequency planar inverted-F antenna, IEEE Trans Antennas Propag 45 (1997), 1451–1458.
5. Y.X. Guo and H.S. Tan, New compact six-band internal antenna, IEEE Antennas Wireless Propag Lett 3 (2004), 295–297.
6. Y.B. Known, J.I. Moon, and S.O. Park, An internal triple-band planar inverted-F antenna, Electron Lett 2 (2003), 341–344.
7. C.W. Chiu and F.L. Lin, Compact dual-band PIFA with multi-resonators, Electron Lett 38 (2002), 538–540.
8. Z. Li and Y. Rahmat-Samii, Optimization of PIFA-IFA combination in handset antenna designs, IEEE Trans Antennas Propag 53 (2005), 1770–1778.
9. P. Nepa, G. Manara, A.A. Serra, and G. Nenna, Multiband PIFA for WLAN mobile terminals, Electron Lett 4 (2005) 349–350.
10. C.T.P. Song, P.S. Hall, H. Ghafouri-Shiraz, and D.Wake, Triple band planar inverted F antennas for handheld devices, Electron Lett 36 (2000), 112–114.
11. C.A. Balanis, Antenna theory: Analysis and design, Wiley, New York, 1997.
12. J.S. Colburn, Y. Rahmat-Samii, M.A. Jensen, and G.J. Pottie, Evaluation of personal communications dual-antenna handset diversity performance, IEEE Trans Vehicle Technol 47 (1998), 737–746.
13. M.A. Jensen and Y. Rahmat-Samii, FDTD analysis of PIFA diversity antennas on a hand-held transceiver unit, IEEE Antennas Propag Symp Dig (1993), 814–817.
14. D.W. Browne, M. Manteghi, M.P. Fitz, and Y. Rahmat-Samii, Antenna topology impacts on measured MIMO capacity, In: Proceedings of IEEE Vehicular Technology Conference, September 2005.
15. M. Manteghi, Y. Rahmat-Samii, Multiport characteristics of a wideband cavity backed annular patch antenna for multi-polarization operations, IEEE Trans Antennas Propag 53 (2005), 466–474.
16. A. Grau, J. Romeu, F. De Flaviis, On the diversity gain using a butler matrix in fading MIMO environments, In: Proceedings of IEEE/ACES international conference on wireless communications and applied computational electromagnetics, 2005, pp. 478–481.
17. Y. Gao, C.C. Chiau, X. Chen, and C.G. Parini, Modified PIFA and its array for MIMO terminals, IEEE Microwaves Antennas Propag Proc 152 (2005), 255–259.
18. D.W. Browne, M. Manteghi, M.P. Fitz, and Y. Rahmat-Samii, Experiments with compact antenna arrays for mimo radio communications, IEEE Trans Antennas Propag, submitted.

THE HIGH ISOLATION DUAL-BAND INVERTED F ANTENNA DIVERSITY SYSTEM WITH THE SMALL N-SECTION RESONATORS ON THE GROUND PLANE

Ki-Jin Kim and Kwang-Ho Ahn
Korea Electronics Technology Institute Wireless Components and Telecommunication Research Center, Bundang-gu, Sungnam-si, Republic of South Korea

Received 23 July 2006

ABSTRACT: *The high isolated dual-band inverted-F diversity systems for portable devices, operating in 2.4 GHz band (2400–2484 MHz) and 5.2 GHz band (5150–5350 MHz), are presented. To reduce the mutual coupling and get high isolation between two internal dual-band antennas, we proposed the small N-section resonators in the form of slots on the ground plane. The optimized small size resonators for high isolation, antenna radiation efficiency, and high effective diversity are analyzed. Because of their small size, N-section resonators can be widely used in small diversity systems that require high isolation between antennas.*
 Microwave Opt Technol Lett 49: 731–734, 2007; Published online in Wiley InterScience (www.interscience.wiley.com). DOI 10.1002/mop.22238

Key words: *high isolation; antenna diversity; MIMO antenna*

1. INTRODUCTION

With the rapid spread of Internet, broadband communication access such as wireless local area network has been studied actively during the past decades to increase the quantities of the data and improve the quality of the information. However, signal fading due to the multi-path propagation is an additional factor that impairs the capacity in the wireless communication. The use of multielement antennas, such as multi input multi output (MIMO) systems, is one of the effective ways for improving reliability and increasing the capacity of the channel [1]. The capacity of the wireless channels is affected by the mutual coupling between the antenna-elements [2]. So, high isolation between antenna-elements, which enables the receiver to receive uncorrelated signals even though antennas are closely spaced, is required for MIMO terminals. In portable devices, two to four antenna-elements are considered and the restricted available area for antennas is an open issue. Recently, many studies on reducing mutual coupling between two antennas—two 2.4 GHz/5.2 GHz dual-band antenna with the reflector [3–4], two 5.2 GHz single antennas with the additional ground plane [5], two 5.2 GHz single antennas with a single $\lambda/4$ slot [6]—have been presented.

In this article, we present a study of two internal dual band WLAN antennas with the small N-section resonators on the ground plane for a PDA phone. In this study, dual-band WLAN antenna, operating in 2.4 GHz band (2400–2480 MHz) and 5.2 GHz band (5150–5350 MHz), is printed in the form of inverted F antenna (IFA) with compact size (Fig. 1) and is suitable to be mounted at the top and side edge of the system circuit board as internal antennas.

2. THE ANTENNA AND SMALL N-SECTION RESONATORS DESIGN

The geometry and dimensions of the investigated configuration are depicted in Figure 1. As a basic antenna element for multi-element antennas, the IFA is considered because the shorting strip of IFA would function as a reflecting metal plate [6]. The antennas are